Morphology and Nonisothermal Crystallization Behavior of PP/Novolac Blends

Limei Cui, Shifeng Wang, Yong Zhang, Yinxi Zhang

Research Institute of Polymer Materials, School of Chemistry and Chemical Technology, Shanghai Jiao Tong University, Shanghai 200240, China

Received 27 April 2006; accepted 16 December 2006
DOI 10.1002/app.25948
Published online 15 March 2007 in Wiley InterScience (www.interscience.wiley.com).

ABSTRACT: The morphology and nonisothermal crystallization behavior of PP/Novolac blends were studied with scanning electron microscopy, differential scanning calorimeter, polarized optical microscopy (POM), and wide-angle X-ray diffraction (WAXD). The results showed that the crystallization of PP in PP/Novolac blends was strongly influenced by cooling rate, size of Novolac particles, crosslinking, and compatibilizer maleic anhydride-grafted PP (MPP). In dynamically cured PP/MPP/Novolac blends, the MPP grafted on the surface of cured Novolac particles and formed a chemical linkage through the reaction of anhydride groups with the hexamethylenetetramine. The graft copolymer not only improved interfacial compatibility but also acted as an effective heterogeneous nucleating agent, which accelerates the crystallization of PP. The combination of Avrami and Ozawa equations exhibited great advantages in treating the nonisothermal crystallization kinetics in dynamically cured PP/MPP/Novolac blends. The POM results showed that the spherulite morphology and the size of PP in PP/MPP/Novolac blends were greatly affected by Novolac. WAXD experiment demonstrates that the PP and dynamically cured PP/MPP/Novolac blends showed only the α crystal form. At the same time, the addition of Novolac resin also affects the crystal size of PP. © 2007 Wiley Periodicals, Inc. J Appl Polym Sci 105: 379–389, 2007

Key words: PP; Novolac resin; dynamic cure; crystallization

INTRODUCTION

Polypropylene (PP) is a commodity polymer used in large quantities in all fields of application. However, it exhibits a relatively low modulus and stiffness compared with the engineering plastics. Glass fiber and inorganic fillers are frequently used to enhance the stiffness, modulus, and dimensional stability of PP.[1,2] Besides using traditional techniques, various additional attempts are used to improve the properties and widen the application field. Dynamic vulcanization is an effective way to prepare thermoplastic vulcanizates.[3–5] Previously, Jiang et al.[6] applied dynamic vulcanization to thermoplastic resin/thermosetting resin (PP/epoxy) blends, which increased the modulus and stiffness of PP. Therefore, PP/Novolac system was further studied. As the Novolac resin and PP are immiscible, maleic anhydride-grafted PP (MPP) was used as a compatibilizer. Experimental results showed that the dynamically cured PP/MPP/Novolac blend had better mechanical properties than that of uncured PP/Novolac blend, uncured PP/MPP/Novolac, and dynamically cured PP/Novolac blends. The dynamic cure of Novolac led to an improvement in the modulus and stiffness of the PP/Novolac blends. The addition of MPP into dynamically cured PP/Novolac blend further led to an obvious improvement in the mechanical properties. With increasing Novolac content, the tensile strength, flexural modulus, and flexural strength increased significantly, whereas the elongation at break dramatically decreased.

PP is a semicrystalline polymer. The final mechanical properties of composites based on PP depend strongly on the microstructure and crystal structure, which in turn depend on the processing condition. Therefore, it is necessary to understand the relationship between processing condition and the development, nature, and degree of crystallinity of PP composites.[7] To control the rate of crystallization and the degree of crystallinity, a great deal of efforts has been devoted to studying the crystallization kinetics and determining the change in material properties.[8] Xu et al.[9] studied the crystallization kinetics of PP with hyperbranched polyurethane acrylate (HUA), which acted as a toughening agent. The addition of HUA increased the number of effective nuclei and the crystallization rate. Seo et al.[10] found that the presence of MPP in isotactic PP affects the crystallization of PP by acting as a nucleating agent. Nano-fillers were also used as more effective nucleating agents for PP crystallization.[11,12] Generally, the smaller the dispersed particles are, the more effective the nucleating agents for PP crystallization. Papageorgiou et al.[13] studied

Correspondence to: Y. Zhang (yxzhang@sjtu.edu.cn).

Journal of Applied Polymer Science, Vol. 105, 379–389 (2007)
© 2007 Wiley Periodicals, Inc.

the isothermal and nonisothermal crystallization kinetics of PP/surface-treated SiO_2 nanocomposites. It was found that Ozawa analysis was rather inapplicable for the nanocomposites. However, the modified Avrami method as well as the method proposed by Mo gave satisfactory results.

However, to our knowledge, the crystallization kinetics for crystalline polymers and crosslinked thermosetting blends has drawn relatively little attention. In such a system, crystallization becomes very complicated. Zhong and Guo[14] have studied crystallization kinetics of miscible thermosetting polymer blends of Novolac resin and poly(ethylene oxide) (PEO). The addition of noncrystlline component into PEO caused a depression in both the overall crystallization rate and the melting temperature. Curing led to the increase of the overall crystallization rate of the blends, and enhanced the nucleating rate of PEO. Guo and Groeninckx[15] have studied isothermal crystallization kinetics of poly(ε-caprolactone) (PCL) in miscible thermosetting polymer blends of epoxy resin and PCL. The influence of curing on the crystallization and melting behavior of PCL is rather complicated. And curing led to the increase of the overall crystallization rate of the blends, and enhanced the nucleation rate of PCL. Jiang et al.[16] have investigated the crystallization behavior of PP in dynamically cured PP/epoxy blends. The nonisothermal crystallization parameters showed that epoxy particles in the PP/epoxy blends can act as effective nucleating agents, accelerating the crystallization of PP component in the PP/epoxy blends. The smaller the epoxy particles in dynamically cured PP/epoxy blends, the more effective for the nucleating. The kinetics of the isothermal crystallization of dynamically cured PP/epoxy blends can be described by the Avrami equation.

In this article, the nonisothermal crystallization and morphology of PP in dynamically cured PP/MPP/Novolac blends was further studied. The size of PP spherulites in the blends was also studied. Crystallization kinetic parameters based on the nonisothermal crystallization of the PP and blends were calculated according to the Ozawa and Combined Avrami equation and Ozawa method. The effect of MPP and Novolac on the crystallization behavior of PP in blends was analyzed.

EXPERIMENTAL

Materials

PP (F401) was produced by Liaoning Panjin Petrochemical (China), with a melt flow index (MFI) of 2.3 g/10 min (230°C, 2.16 kg). The Novolac resin was purchased from Qinan Adhesive Materials Factory (China). MPP with a MAH content of 1% (w/w) was prepared by Shanghai Sunny New Technology Development (China). The curing agent, hexamethylenetetramine (HMTA), was produced by Shanghai Chemical Agent Company (China).

Sample preparation

Before blending, MPP and the Novolac resin were dried at 70°C under vacuum for about 12 h. Dynamically cured PP/Novolac blends were prepared in the mixing chamber of a Haake Rheometer RC90 at 190°C and 50 rpm. MPP and PP were first mixed for 2 min, then the Novolac resin was added. After 2 min, the curing agent (HMTA) was added under continuous mixing. The total mixing process lasted 10 min. The composition was moved out and compression-molded in a press at 190°C for 20 min, then cold pressed to get samples for testing.

Scanning electron microscopy

Morphologies of the blends were studied using scanning electron microscopy (SEM) (HITACHI-*S*-2150). SEM micrographs were taken from cryogenically fractured surfaces of blend specimens. The fractured surfaces of PP/Novolac blends were etched by acetone for 10 h at room temperature, to remove the Novolac resin phase of uncured PP/Novolac blends and to dissolve the soluble part of the Novolac resin of cured PP/Novolac blends, and then coated with gold for further observation. The number-average particle diameter (d_n) was calculated from a minimum of 200 particles as $d_n = \sum n_i d_i / \sum n_i$, where n_i is the number of particles with a diameter d_i.

Differential scanning calorimetry analysis

Thermal analysis of the PP/Novolac blends was performed using a Perkin–Elmer differential scanning calorimeter (DSC). All tests were performed in a nitrogen atmosphere with a sample weight of about 4 mg. All samples were first heated to 200°C at 20°C/min and kept for 5 min to eliminate prior thermal history. The specimen was subsequently cooled down to 30°C at a cooling rate of 2.5, 5, 10, or 20°C/min and then heated to 200°C at 10°C/min for data collection.

Polarized optical microscope analysis

The size of PP spherulites was studied on thin films by using a polarized optical microscope (POM) LEICA-DMLPl, with an automatic hot-stage thermal control. A sample was sandwiched between microscope cover glasses, melted at 200°C for 5 min, and then rapidly cooled to 150°C for isothermal crystallization

for 1 h. The PP spherulites were observed in micrographs taken at appropriate intervals.

Wide-angle X-ray diffraction

A sample with the thickness of 1 mm was scanned by a speed of 4°/min at ambient temperature using an X-ray diffractometer (SA-HF3; Rigaku, Japan) with Cu Kα radiation (λ = 0.154 nm) at a generator voltage of 40 kV and a current of 40 mA.

RESULTS AND DISCUSSION

Morphology of PP/Novolac blends

Figure 1 shows the SEM micrographs of the fracture surfaces of PP/Novolac blends. For the PP/Novolac

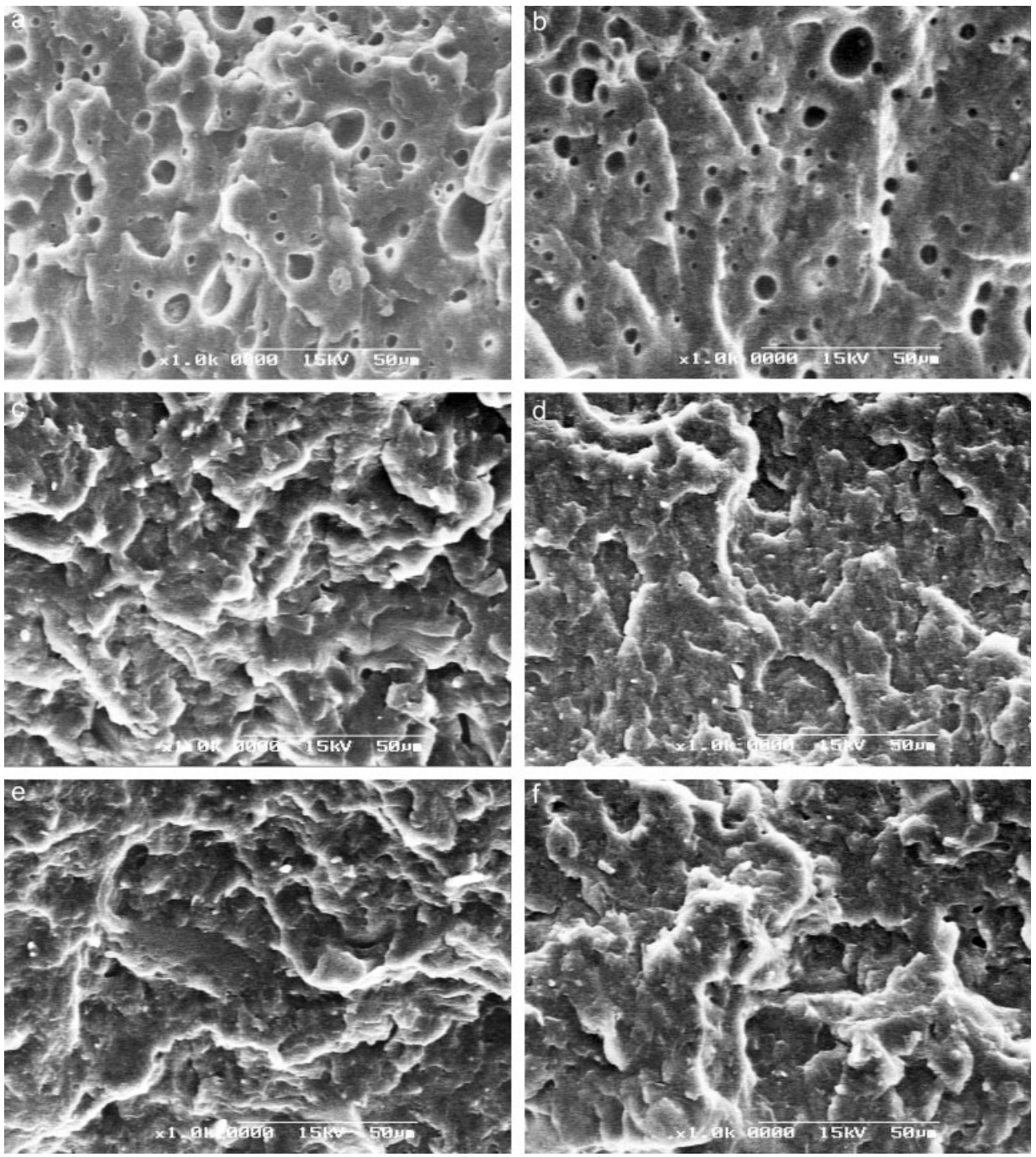

Figure 1 SEM micrographs of PP/Novolac blends: (a) PP/Novolac (90/10); (b) PP/MPP/Novolac (80/10/10); (c) PP/Novolac/HMTA (90/10/1); (d) PP/MPP/Novolac/HMTA (80/10/10/1); (e) PP/MPP/Novolac/HMTA (60/10/30/3); (f) PP/MPP/Novolac/HMTA (40/10/50/5).

(90/10) blend [Fig. 1(a)], the Novolac resin is dispersed as spherical particles with an average diameter of about 3.7 μm in the PP matrix, and the boundaries between the dispersed phase and the PP matrix are distinct. For the PP/MPP/Novolac (80/10/10) blend [Fig. 1(b)], Novolac particles with an average diameter of about 3.3 μm are distributed in the PP matrix, and the size of particles is similar to that of PP/Novolac blend. This suggests that MPP cannot evidently improve the compatibility between PP and the Novolac resin and promote a more fine dispersion of the Novolac phase, although there is the action of hydrogen bonding between the hydroxyl groups of Novolac and the carbonyl groups of MAH.

Figure 1(c) shows the fracture surfaces of dynamically cured PP/Novolac blend. The cured Novolac resin is dispersed as particles in the PP matrix and the average diameter of the particles is about 3.0 μm. As shown in Figure 1(d–f), the addition of MPP into dynamically cured PP/Novolac blends decreases evidently the average diameter of the Novolac particles. The average diameter of the particles slightly increases with increasing Novolac resin content. The average diameter of the Novolac particles is about 0.7, 0.9, and 1.5 μm, respectively, for the PP/MPP/Novolac/HMTA blends with increasing Novolac resin content. It indicates that the dynamic cure of the Novolac resin can prevent the Novolac particles from aggregation in the PP matrix and result in finer domains in dynamically cured PP/MPP/Novolac blends. Furthermore, it suggests that the addition of MPP improve the dispersion and interfacial adhesion. For the cured PP/MPP/Novolac blends, the compatibilizer MPP grafted on the surface of Novolac particles and formed a chemical linkage through the reaction of anhydride groups with the HMTA. The formation of the graft copolymer has been confirmed though solvent extraction. Consequently, the compatibilizer molecules chemically graft to the Novolac phase during curing process. The graft copolymers preferentially reside at the interface, reduce interfacial tension, and improve interfacial adhesion.

Nonisothermal crystallization of the PP/Novolac blends

Figure 2 shows the DSC thermograms of the PP and PP/Novolac blends at a cooling rate of 10°C/min. For PP, PP/MPP, and all PP/Novolac blends, only a single crystallization peak can be seen. In all cases, the peak temperature, T_p, which corresponds to the maximum crystallization rate, shifts to higher temperature compared with that of PP (111.6°C).

As shown in Figure 2(a), T_p of the PP in PP/MPP (90/10) is increased by about 7°C compared with PP, which is similar to that of PP/Novolac (90/10) blend. Thus, the MPP and Novolac resin are effective nucleating agents for PP crystallization. Moreover, the addition of compatibilizer MPP into PP/Novolac blend cannot further enhance T_p of PP compared with that of PP/Novolac blend. However, cured Novolac resin can evidently increase the T_p of PP compared with that of uncured Novolac and MPP. And dynamically cured PP/MPP/Novolac/HMTA (80/10/10) blend has the highest T_p (128.9°C). At the same time, it can be seen that the T_p of the PP in dynamically cured PP/MPP/Novolac decreases with increasing Novolac resin content.

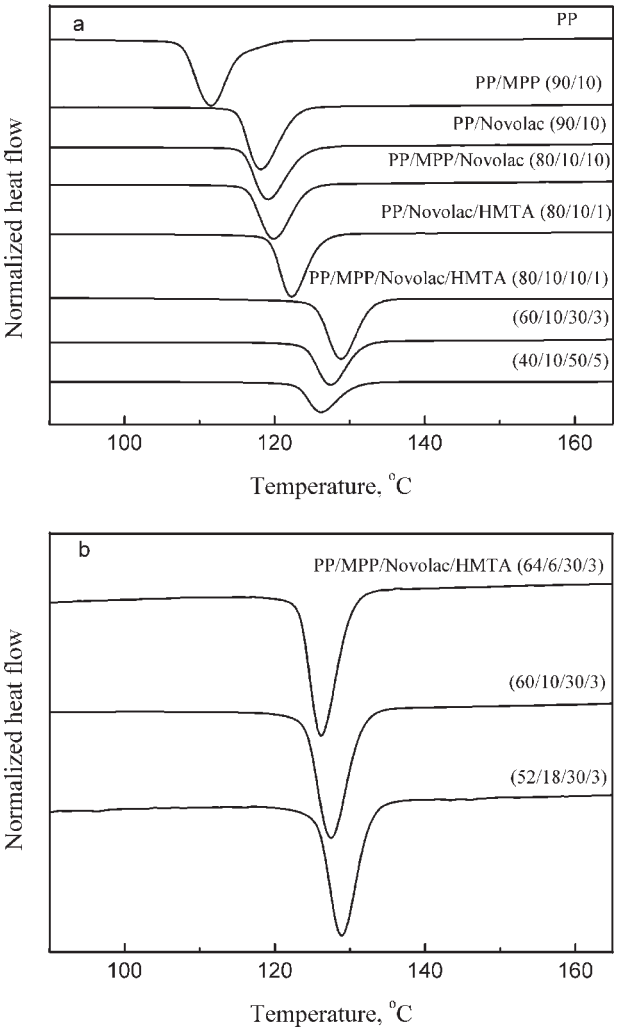

Figure 2 Normal DSC thermograms for (a) PP, PP/MPP, and PP/Novolac blends and (b) dynamically cured PP/MPP/Novolac blends prepared by nonisothermal crystallization at a cooling rate of 10°C/min.

The results show that all uncured and cured Novolac particles in the PP/Novolac blends can act as effective nucleating agents, accelerating the crystallization of PP component in the blends. Both the curing process and compatibilizer remarkably enhance the overall crystallization rate of the blend. The results can be interpreted by the size of Novolac particles. Generally, the smaller the dispersed particles

are, the more effective the nucleating agents for PP crystallization. In addition, the graft copolymer with segments of MPP and Novolac can be regarded as the most effective heterogeneous nucleation agent of PP crystallization compared with MPP, Novolac, and cured Novolac resin.

The influence of MPP content on dynamically cured PP/MPP/Novolac blends has been investigated, maintaining the content of cured Novolac constant. As shown in Figure 2(b), the T_p of the PP in dynamically cured PP/MPP/Novolac blends increased slightly with increasing MPP content. It suggests that the MPP can affect PP crystallization, but the influence of MPP content on the PP crystallization in blends is not evident. In this case, the results can be explained that with increasing MPP content, more MPP grafted to the surface of cured Novolac particles, which enhances the PP crystallization. It shows that the more the relative amount of MPP grafted on the surface of cured Novolac particle, the more effective the nucleating ability for PP crystallization.

Because the crystallization behavior is strongly dependent on the crystallization speed, the effect of cooling rate on the crystallization behavior of the PP and PP/Novolac blends is investigated. The crystallization data of PP and dynamically cured PP/MPP/Novolac blends are listed in Table I.

For PP and dynamically cured PP/MPP/Novolac blends, the T_p and the onset temperature (T_{onset}, which is the temperature at the intercept of the tangents at the baseline and the high-temperature side of the exotherm) shift to lower temperature with increasing cooling rate. It also shows that the lower cooling rate has the earlier crystallization starts. The decrease in T_p, with a faster cooling rate, was a result of the crystallization rate being slower than the experimental cooling rate.[17] Besides, as the cooling rate increases, the crystallized fraction may consist of defective crystals as a result of higher supercooling.[18]

As seen in Table I, all T_ps of PP in the dynamically cured PP/MPP/Novolac blends are higher than that of PP at the same cooling rate. It is because that the MPP grafting copolymer can easily absorb the PP chain segments, and therefore, the crystallization of PP molecules can occur at a higher crystallization temperature. Moreover, the T_p of PP in dynamically cured PP/MPP/Novolac blends shifts to lower temperature with increasing Novolac content. As MPP content in blends is constant, the results can be interpreted that the relative amount of grafted MPP on the surface Novolac particles decrease with increasing the Novolac content, which leads to the nucleating activity of graft copolymer decreases. It is demonstrated further by activation energy of crystallization for dynamically cured PP/MPP/Novolac blends.

TABLE I
Nonisothermal Crystallization Parameters of PP and Dynamically Cured PP/MPP/Novolac Blends at Different Cooling Rates

Composition	ϕ (°C/min)	T_{onset} (°C)	T_p (°C)	$T_{1/2}$ (min)
PP	2.5	123.0	116.8	33.1
	5	117.5	114.3	17.3
	10	115.6	111.6	9.01
	20	113.3	108.2	4.70
PP/MPP/Novolac/ HMTA (80/10/10/1)	2.5	139.7	136.2	25.9
	5	136.2	132.7	13.7
	10	132.8	128.9	7.31
	20	129.8	124.9	3.89
PP/MPP/Novolac/ HMTA(60/10/30/3)	2.5	137.6	134.3	26.6
	5	134.7	131.0	14.0
	10	131.6	127.5	7.47
	20	128.1	123.6	3.96
PP/MPP/Novolac/ HMTA(40/10/50/5)	2.5	137.0	133.0	27.1
	5	134.2	129.5	14.3
	10	130.6	126.2	7.54
	20	127.8	122.3	4.01

Nonisothermal crystallization kinetics analysis

For nonisothermal crystallization, the relative degree of crystallinity, *X(T)*, which is a function of crystallization temperature, can be defined as

$$X(T) = \int_{T_0}^{T} (dH/dT)\, dT / \int_{T_0}^{T\infty} (dH/dT)\, dT \qquad (1)$$

where T denotes the crystallization temperature at time t, T_o and T_∞ are the initial and end of crystallization temperature, respectively. Figure 3 shows the relative crystallinity of PP and dynamically cured PP/MPP/Novolac blend (80/10/10) at various cooling rates. All curves in Figure 3 shows the same sigmoidal shape, implying the lag effect of the cooling rate on crystallization. The plot of *X(T)* versus T shifts to the low-temperature region as the cooling rate increases. The slower cooling rate provided more fluidity and diffusivity for the molecules because of the relativity lower viscosity and more time for perfection crystallization, thus inducing much higher crystallinity at higher temperature than for the samples cooled with fast cooling rates.[19] The relation between the crystallization time t and the sample temperature T can be formulated as

$$t = (T_0 - T)/\Phi \qquad (2)$$

where Φ is the cooling rate. According to eq. (2) the abscissa of temperature in Figure 3 could be transformed into a timescale. It is clear that the higher the cooling rate is, the shorter the time needed for the completion of the crystallization process. For PP and dynamically cured PP/MPP/Novolac/HMTA blends, the half-times of nonisothermal crystallization, $t_{1/2}$, are listed in Table I. As expected, the value of $t_{1/2}$

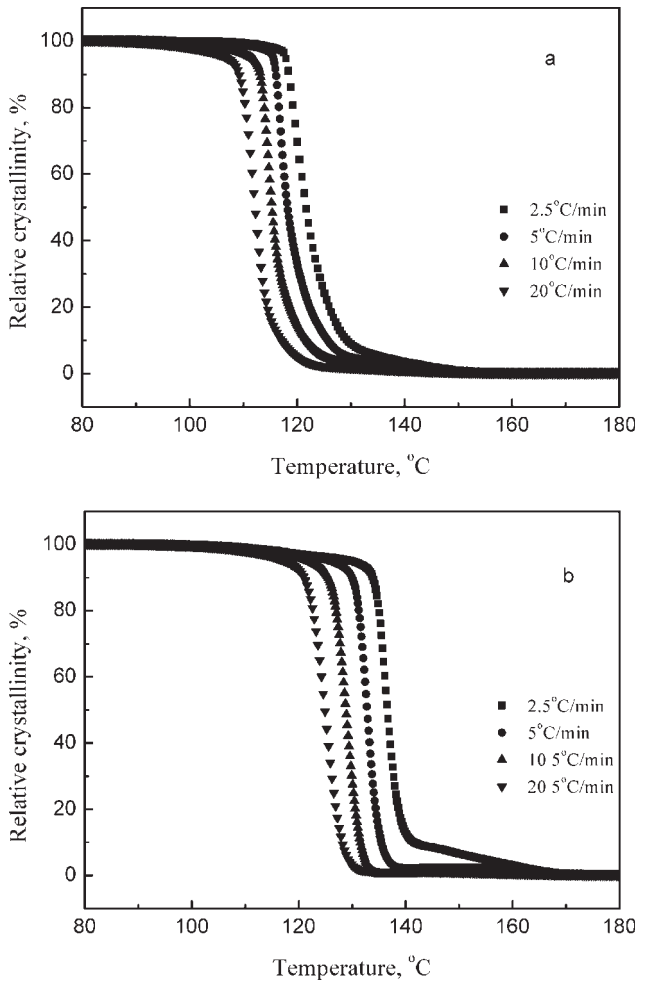

Figure 3 Development of relative crystallinity with temperature for nonisothermal crystallization: (a) PP; (b) PP/MPP/Novolac/HMTA (80/10/10/1).

decreased with increasing cooling rate for PP and PP/MPP/Novolac/HMTA blends. Moreover, the value of $t_{1/2}$ for dynamically cured PP/MPP/Novolac blends was evidently lower than that of PP at a given cooling rate, indicating that the MPP grafting Novolac copolymer could accelerate the overall crystallization process. And it is also seen that the value of $t_{1/2}$ for dynamically cured PP/MPP/Novolac blends increased slightly with increasing Novolac content at the same cooling rate. The results show that the more the dynamically cured Novolac content, the slower the crystallization rate. It can be interpreted that the relative amount of MPP grafting on the surface of Novolac phase decreases with increasing Novolac content, which is further interpreted by activation energy of crystallization for PP/Novolac blends.

Ozawa model

Considering the effect of cooling rate on the nonisothermal crystallization, Ozawa[20,21] extended the Avrami theory from isothermal crystallization to nonisothermal crystallization by assuming that the nonisothermal crystallization process was composed of infinitesimally small isothermal crystallization steps. According to Ozawa theory, the relative crystallinity $X(T)$, at temperature T, can be calculated as:

$$X(T) = 1 - \exp\left(-\frac{K^*(T)}{\Phi^m}\right) \quad (3)$$

where $K^*(T)$ is the function of cooling rate related to the all over crystallization rate, Φ is the cooling rate, and m is the Ozawa exponent that depends on the dimension of crystal growth. Similarly, the eq. (3) can be changed to its linear form:

$$\log[-\ln(1 - X(T))] = \log K^*(T) - m \log \Phi \quad (4)$$

If the Ozawa method is valid, by plotting $\log[-\ln(1-X(T))]$ against $\log \Phi$ at a given temperature, a straight line should be obtained. Thus, $K^*(T)$ and m could be estimated from the intercept and slope, respectively. The results based on the Ozawa method are illustrated in Figure 4.

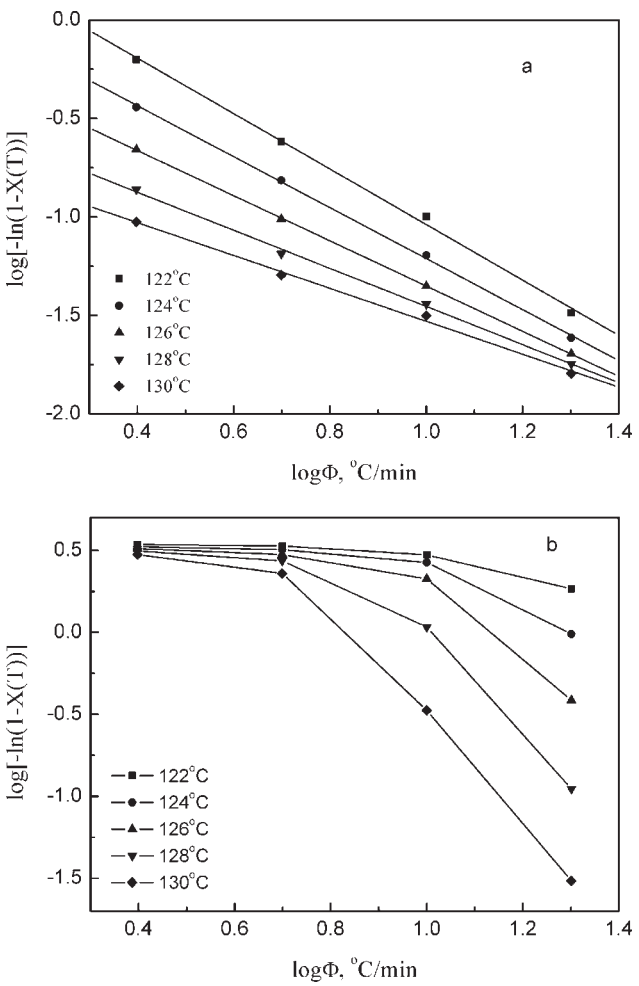

Figure 4 Ozawa plots of $\log[-\ln(1 - X(T))]$ versus $\log \Phi$ at indicated temperature for PP and dynamically cured PP/MPP/Novolac blends; (a) PP; (b) PP/MPP/Novolac/HMTA (80/10/10/1).

TABLE II
Nonisothermal Crystallization Kinetic Parameters for PP at Different Temperature

Temperature (°C)	*m*	*K(T)*
122	1.41	2.34
124	1.29	1.21
126	1.15	0.63
128	0.97	0.33
130	0.83	0.20

Figure 4 illustrates the plots of $\log[-\ln(1-X(T))]$ as a function of $\log \Phi$. In the case of PP, the curves exhibit a better linear relationship, but clearly no straight lines for dynamically cured PP/MPP/Novolac blends are observed. The results show that PP can be analyzed by the Ozawa method but that dynamically cured PP/MPP/Novolac blends cannot. The reason for the difference is that the crystallization processes for dynamically cured PP/MPP/Novolac are at different stages at different cooling rates at a given temperature; that is, the lower cooling rate process is toward the end of the crystallization process, whereas the higher cooling rate process is at an early stage of the crystallization process. The addition of cured Novolac magnifies the influence of cooling rate on the crystallization process.[7] In addition, large amount of crystallization occurs as a result of secondary processes, leading to the deviation from the straight lines.

The nonisothermal crystallization kinetic parameters for PP at different temperature are listed in Table II. As shown in Table II, the values of the Ozawa exponent are not integers and are between 0.8 and 1.4 for pure PP, which is comparable with that obtained by Li et al.[22] (1.4–2.4) and obtained by Xu et al.[9] (1.0–1.2).

Combined Avrami equation and Ozawa equation

It is evident that in several cases both the Avrami equation and the Ozawa equation are inadequate in analysis of nonisothermal crystallization of the polymers. Several semitheoretical mathematical models based on the Avrami equation have been proposed in the literature.[23–25] Lou and Mo[26] proposed a novel kinetics equation by combining Avrami and Ozawa equations to exactly describe the nonisothermal crystallization process. On the basis of the following assumption: the crystallinity is correlated to both the cooling rate and the crystallization time and consequently for particular crystallinity these two parameters can be derived by combining the Avrami and Ozawa equations.

The Avrami equation in double logarithmic form is expressed as

$$\log[-\ln(1 - X(t))] = \log K + n \log t \qquad (5)$$

where n is the Avrami exponent whose value depends on the mechanism of nucleation and on the form of crystal growth, and K is constant containing the nucleation and growth parameters. Based on eqs. (1) and (2), Avrami equation can be used for nonisothermal crystallization analysis as follows:

$$\log[-\ln(1 - X(t))] = \log Z_t + n \log t \qquad (6)$$

where the exponent n is a mechanism constant that depends on the type of nucleating and growth process parameters, and Z_t is a composite rate constant involving both nucleating and growth rate parameters. Thus, connecting eqs. (4) and (6), the following equation can be obtained at a given crystallinity degree:

$$\log \Phi = \log F(T) - \mathrm{a} \log t \qquad (7)$$

where $a = \frac{n}{m}$ (ratio of Avrami exponent and the Ozawa exponent), and $F(T) = [\mathrm{K}*(T)/Z_t]^{\frac{1}{m}}$ means the necessary values of cooling rate to reach a defined degree of crystallinity at unit crystallization time. According to eq. (7), at a given degree of crystallinity, the plot of $\log \Phi$ as a function of $\log t$ gives a straight line, and $\log F(T)$ and a are determined from the intercept and slope.

Figure 5 presents plots of $\log \Phi$ versus $\log t$ at various degree of crystallinity for PP and dynamically cured PP/MPP/Novolac blends. $\log F(T)$ and a derived from the intercept and slope of the plots are listed in Table III. The deviation of the values of a for PP and dynamically cured PP/MPP/Novolac blends is very small, indicating that eq. (7) can be successfully used to describe the nonisothermal crystallization of PP in dynamically cured PP/MPP/Novolac blends. As can be seen in Table III, the values of $\log F(T)$ increase with increasing relative crystallinity, indicating that at an unit crystallization time, a higher cooling rate should be required to obtain a higher degree of crystallinity. Nevertheless, the values of the parameter α are almost constant.

Crystallization activation energy

In the case of a nonisothermal crystallization experiment using DSC, the effective activation energy ΔE can be evaluated from Kissinger method.[27] Taking into account the variation of the peak temperature T_p with the cooling rate Φ' the effective activation energy ΔE can be evaluated based on plots of the following form:

$$\frac{d\left[\ln \Phi/T_p^2\right]}{d(1/T_p)} = -\frac{\Delta E}{R} \qquad (8)$$

where R is the gas constant. Figure 6 illustrates plots based on the Kissinger method. And it can be seen that good linear relations are obtained. From the

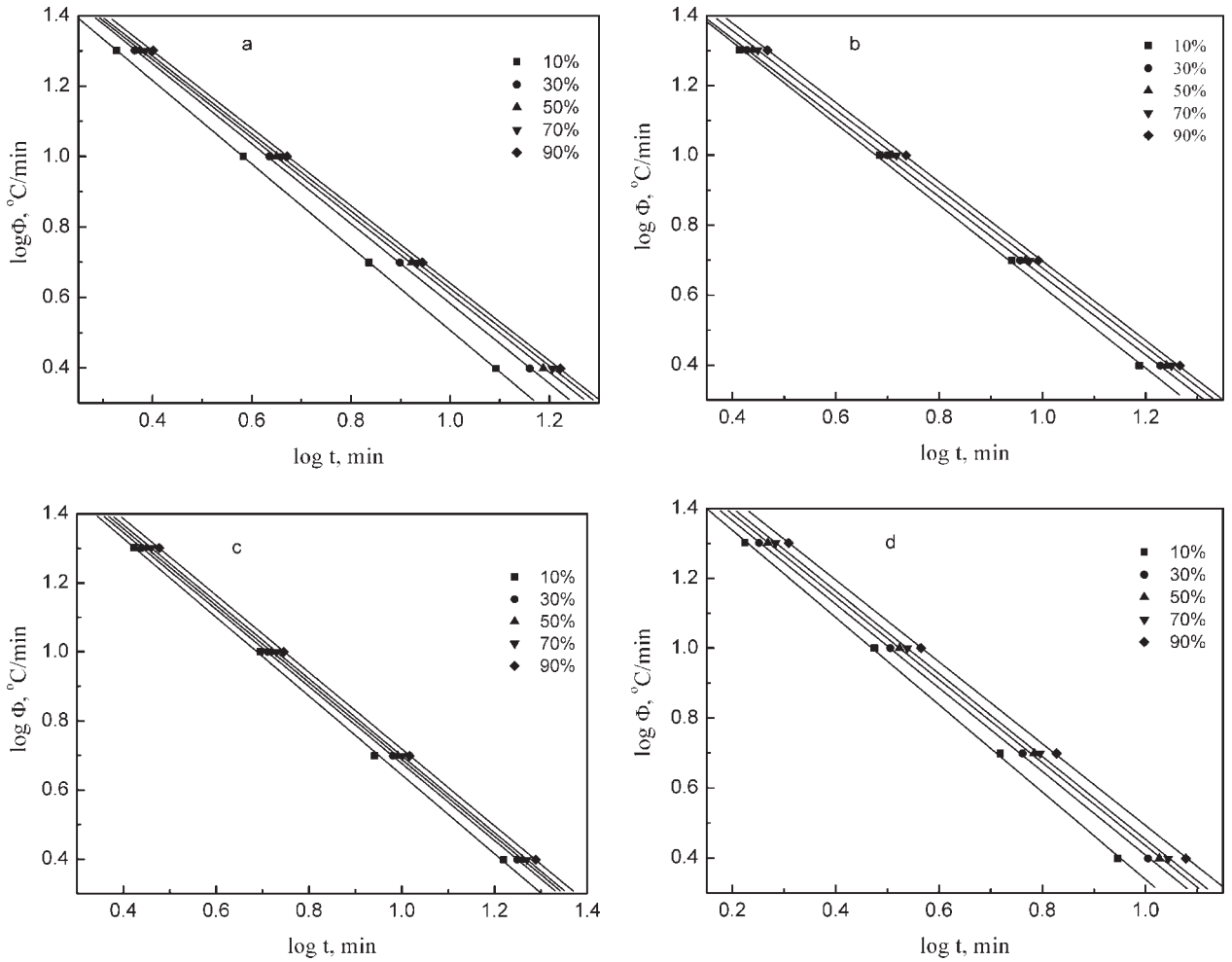

Figure 5 Plots of log Φ versus log *t* for PP and dynamically cured PP/MPP/Novolac blends. (a) PP; (b) PP/MPP/Novolac/HMTA (80/10/10/1); (c) PP/MPP/Novolac/HMTA (60/10/30/3); (d) PP/MPP/Novolac/HMTA (40/10/50/5).

slopes of the curves, the effective activation energy ΔE can be calculated accordingly. The calculated values of the activation energy obtained are listed in Table III. As can be seen, the ΔE of neat PP is greater than that of dynamically cured PP/MPP/Novolac blends, suggesting the crystal growth of dynamically cured PP/MPP/Novolac blends is easier than that of pure PP. And it also be seen that the value of

TABLE III
Nonisothermal Crystallization Kinetics Parameters from Combination of Avrami-Ozawa Equation for PP and Dynamically Cured PP/MPP/Novolac Blends

		X_t (%)				
Samples	Parameters	10	30	50	70	90
PP	*a*	1.18	1.13	1.11	1.10	1.10
	log *F(t)*	1.68	1.71	1.72	1.72	1.74
	ΔE (kJ/m^2)			329.7		
PP/MPP/Novolac/HMTA	*a*	1.17	1.13	1.13	1.13	1.14
(80/10/10/1)	log *F(t)*	1.79	1.79	1.79	1.81	1.83
	ΔE (kJ/m^2)			244.0		
PP/MPP/Novolac/HMTAl	*a*	1.14	1.12	1.11	1.11	1.11
(60/10/30/3)	log *F(t)*	1.79	1.79	1.80	1.81	1.83
	ΔE (kJ/m^2)			255.3		
PP/MPP/Novolac/HMTAl	*a*	1.25	1.20	1.19	1.19	1.17
(40/10/50/5)	log *F(t)*	1.59	1.60	1.62	1.64	1.66
	ΔE (kJ/m^2)			268.2		

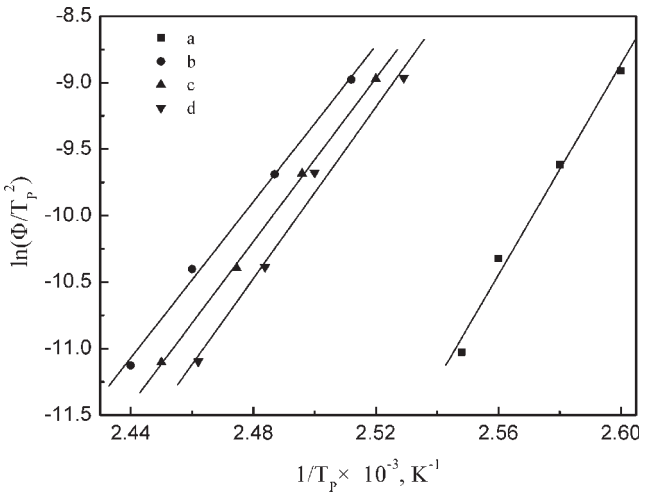

Figure 6 Plots of $\ln(\Phi/T_p^2)$ versus $1/T_p$ for PP and dynamically cured PP/MPP/Novolac blends: (a) PP; (b) PP/MPP/Novolac/HMTA (80/10/10/1); (c) PP/MPP/Novolac/HMTA (60/10/30/3); (d) PP/MPP/Novolac/HMTA (40/10/50/5).

activation energy increased with increasing Novolac content in dynamically cured PP/MPP/Novolac blends, indicating crystal growth of blends is difficult at high Novolac content. It can be explained that the relative amount of grafted MPP on surface of Novolac particles decrease with increasing the Novolac content, as the content of MPP is fixed.

POM and XRD analysis

Figure 7 shows the POM micrographs of PP and dynamically cured PP/MPP/Novolac blends that were isothermally crystallized at 150°C for 1 h. As shown in Figure 7(a), the spherulites of PP are about 100 μm in diameter, which are larger than those of PP in dynamically cured PP/Novolac blends.

With the addition of 10% dynamically cured Novolac, spherulite size promptly decreased, and some spherulites are too small to be seen. The PP molecular chains are more difficult to pack in an ordered manner and a large number of spherulites grow in a limited space. Therefore, perfect spherulites cannot form. And it is also seen that the spherulite size of the PP in the blends slightly increased with increasing Novolac resin content. It indicates that the nucleating activity of Novolac decreased with increasing Novolac content, which is in agreement

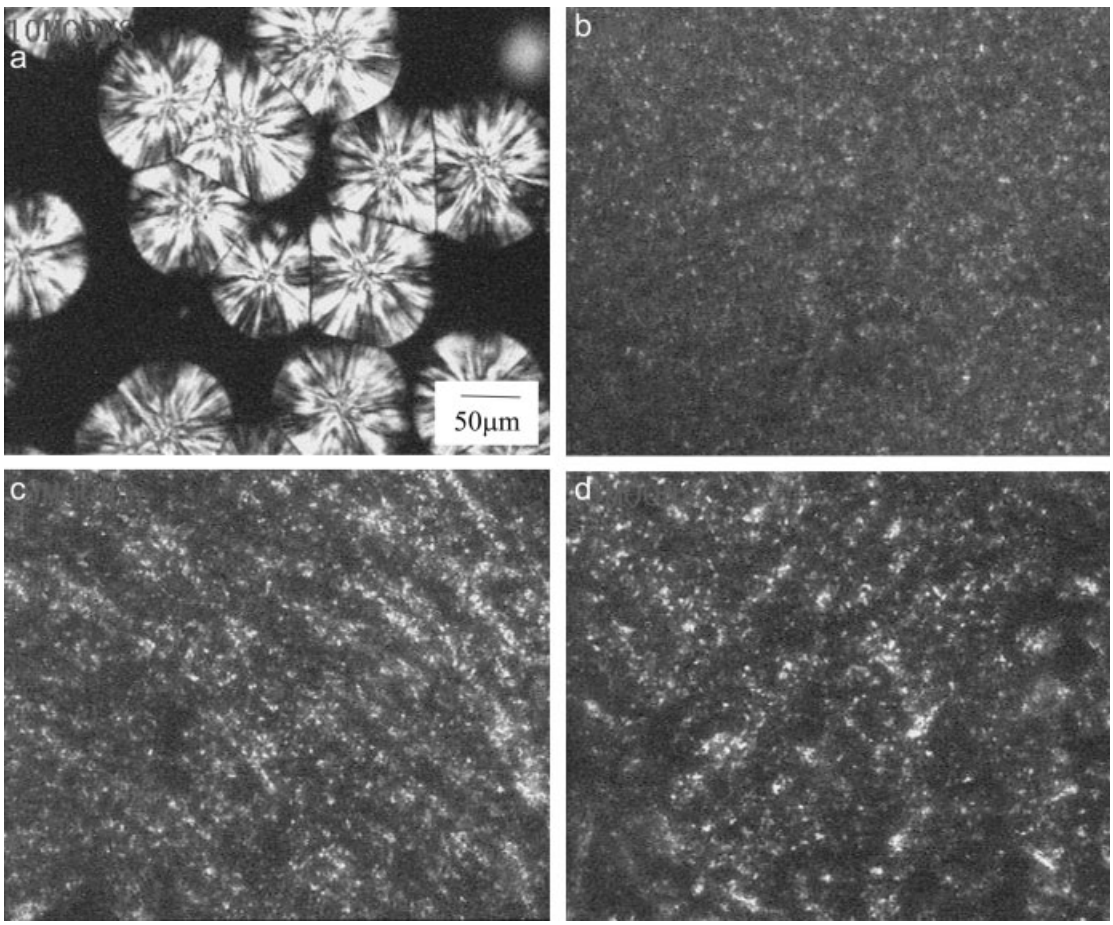

Figure 7 Morphology of crystal by POM (200×). (a) PP; (b) PP/MPP/Novolac/HMTA (80/10/10/1); (c) PP/MPP/Novolac/HMTA (60/10/30/3); (d) PP/MPP/Novolac/HMTA (40/10/50/5).

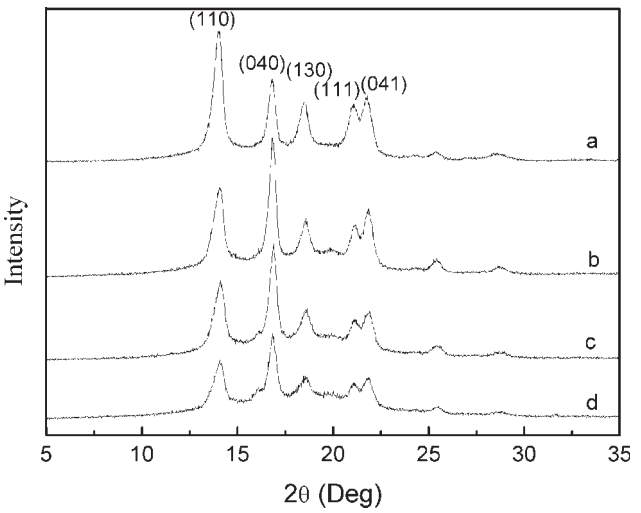

Figure 8 XRD patterns of PP and dynamically cured PP/MPP/Novolac blends. (a) PP; (b) PP/MPP/Novolac/HMTA (80/10/10/1); (c) PP/MPP/Novolac/HMTA (60/10/30/3); (d) PP/MPP/Novolac/HMTA (40/10/50/5).

with the obtained value of crystallization activation energy.

The results showed that the addition of Novolac resin greatly affected the spherulite size and morphology of PP, and the nucleating sites of Novolac particles result in an increase in the number of PP spherulites and reduce the size of the spherulites. Jiang et al.[16] also reported that the addition of the epoxy to the PP matrix could reduce the size of PP spherulites.

The WAXS has been used to investigate the crystalline structure of PP and dynamically cured PP/MPP/Novolac blends. The samples used in X-ray analysis were compression-molded at 190°C for 20 min and cold-pressed at ambient temperature. The X-ray diffractograms of PP and dynamically cured PP/MPP Novolac blends are shown in Figure 8. The strong diffraction peaks were at the diffraction angles 2θ of 14.0°, 16.8°, and 18.6°, of which the three peaks corresponded to (110), (040), and (130) planes, respectively, and were characteristic of the typical α-form monoclinic structure of PP.[28] Figure 8 demonstrates that the PP and their blends prepared from the melt all showed only the α crystal form.

The crystallite size $D_{(hkl)}$ vertical to the lattice plane (*hkl*), can be obtained by Scherrer's equation:[29]

$$D_{(hkl)} = k\lambda/\beta \cos \theta \quad (9)$$

where k is the factor of the crystal figure, λ is the wavelength of the X-ray (λ = 1.541 Å), and θ is the diffraction angle. β is equal to $(B^2 - b_0^2)^{1/2}$, where B is the width at half-tallness of the diffraction peak and b_0 is the broadening factor of the instrument. If we take no account of the lattice distortion, the equation can be simplified as follows:

$$D_{(hkl)} = 0.89\lambda/B \cos \theta \quad (10)$$

TABLE IV
Crystal Size $D_{(hkl)}$ of PP and Dynamically Cured PP/MPP/Novolac Blends

Composition	$D_{(110)}$ (Å)	$D_{(040)}$ (Å)	$D_{(130)}$ (Å)
PP	134.2	189.1	153.1
PP/MPP/Novolac/HMTA (80/10/10/1)	127.7	193.7	151.3
PP/MPP/Novolac/HMTA (60/10/30/3)	114.7	180.5	137.5
PP/MPP/Novolac/HMTA (40/10/50/5)	114.7	172.7	132.7

The crystal size $D_{(hkl)}$ for PP and cured PP/MPP/Novolac blends evaluated for the crystallographic planes (110), (040), and (130) are presented in Table IV. As shown in Table IV, $D_{(110)}$ and $D_{(130)}$ decreased with increasing Novolac content. However, addition of 10% Novolac resin led to an increase in the $D_{(040)}$, further addition of Novolac caused a decrease and reached minimum at Novolac content of 50 wt %. The results showed that the addition of Novolac resin into PP could also affect the crystal size of PP.

CONCLUSIONS

The morphology and nonisothermal crystallization behavior of PP and PP/Novolac blends were studied with SEM, DSC, POM, and wide-angle X-ray diffraction. The results showed that the crystallization of PP in PP/Novolac blends was strongly influenced by cooling rate, size of Novolac particles, crosslinking, and compatibilizer. MPP, uncured and cured Novolac acted as effective heterogeneous nucleating agents, accelerating the crystallization of PP in the PP/Novolac blends. And the smaller the Novolac particles were, the more effective the nucleating agent for PP crystallization. In addition, the MPP-grafted Novolac copolymer can be regarded as a more effective heterogeneous nucleation agent of PP crystallization than MPP, Novolac, and cured Novolac resin. And the more the relative amount of MPP grafts on the surface of Novolac particle, the more effective the nucleating ability for PP crystallization.

The kinetics of nonisothermal crystallization for pure PP could be analyzed by the Ozawa method but that of dynamically cured PP/MPP/Novolac blends could not be properly described. However the combined Avrami and Ozawa equations could be used to describe the nonisothermal crystallization process. The Kissinger method was employed to calculate the activation energy. The activation energy value of neat

PP was greater than that of dynamically cured PP/MPP/Novolac blends. And the value of activation energy increased with increasing Novolac content in dynamically cured PP/MPP/Novolac blends.

The spherulite morphology and size of PP in cured PP/MPP/Novolac blends were greatly affected by Novolac resin. The addition of 10% Novolac resin resulted in a prompt decrease in spherulite size of PP. And it also can be seen that the spherulite size of PP in the blends slightly increased with increasing Novolac resin content. XRD experiment demonstrates that the PP and their blends prepared all showed only the α crystal form. At the same time, addition of Novolac resin also could affect the crystal size of PP.

References

1. Karger, K. J.; Czigany, T. Composites Part A: Appl Sci Manuf 1998, 29, 1319.
2. López-Manchado, M. A.; Arroyo, M. Polymer 2000, 41, 7761.
3. Gessler, M. U.S. Pat. 3,037,954 (1962).
4. Fisher, K. U.S. Pat. 3,758,643 (1973).
5. Coran, A. Y.; Patel, R. P. Rubber Chem Technol 1980, 53, 141.
6. Jiang, X. L.; Huang, H.; Zhang, Y.; Zhang, Y. X. Polym Polym Compos 2004, 12, 29.
7. Xu, W. B.; Liang, G. D.; Wang, W. J Appl Polym Sci 2003, 88, 3093.
8. Weng, W. G.; Chen, G. H.; Wu, D. J. Polymer 2003, 44, 8119.
9. Xu, G.; Shi, W.; Hu, P.; Mo, S. Eur Polym J 2005, 41, 1828.
10. Seo, Y.; Kim, J.; Kim, K. U.; Kim, Y. C. Polymer 2000, 41, 2639.
11. Chan, C. M.; Wu, J. S.; Li, J. X.; Cheung, Y. K. Polymer 2002, 43, 2981.
12. Xu, W. B.; Ge, M. L.; He, P. S. J Polym Sci Part B: Polym Phys 2002, 40, 408.
13. Papageorgiou, G. Z.; Achilias, D. S.; Bikiaris, D. N.; Karayannidis, G. P. Thermochim Acta 2005, 427, 117.
14. Zhong, Z.; Guo, Q. Polymer 2000, 41, 1711.
15. Guo, Q. P.; Groeninckx, G. Polymer 2001, 42, 8647.
16. Jiang, X. L.; Zhang, Y.; Zhang, Y. X. J Polym Sci Part B: Polym Phys 2004, 42, 1181.
17. Park, J. Y.; Kwon, M. H.; Park, O. O. J Polym Sci Part B: Polym Phys 2000, 38, 3001.
18. Cho, K.; Li, F.; Choi, J. Polymer 1999, 40, 1719.
19. Wang, D.; Gao, J. G. J Appl Polym Sci 2006, 99, 670.
20. Ozawa, T. Polymer 1971, 12, 150.
21. Ozawa, T. Polymer 1978, 19, 1142.
22. Li, J.; Zhou, C. X.; Wang, G.; Tao, Y.; Liu, Q.; Li, Y. Polym Test 2002, 21, 583.
23. Ravindranath, K.; Jog, J. P. J Appl Polym Sci 1993, 49, 1395.
24. Lambrigger, M. Polym Eng Sci 1998, 33, 610.
25. Lou, T. X.; Mo, Z. S.; Wang, S. G.; Zhang, H. F. Polym Eng Sci 1997, 37, 568.
26. Lou, T. X.; Mo, Z. S. Acta Polym Sin 1993, 1, 1.
27. Kissinger, H. E. J Res Natl Inst Stan 1956, 57, 217.
28. Tang, J. G.; Wang, Y.; Liu, H. Y.; Belfiore, L. A. Polymer 2004, 45, 2081.
29. Guan, Y.; Wang, S. Z.; Zheng, A.; Xiao, H. N. J Appl Polym Sci 2003, 88, 872.